Heterogeneous Catalysis

DOI: 10.1002/anie.201105922

Detection and Measurement of Surface Electron Transfer on Reduced Molybdenum Oxides (MoO_x) and Catalytic Activities of Au/MoO_x**

Feng Wang, Wataru Ueda, and Jie Xu**

MoO_x is widely used as a catalyst, sensor, electrochemical device, and display material.[1] It is considered that surface defect sites play a key role in most of catalytic applications, either as active centers or as anchoring sites for supported particles.[2] The evolution of defect sites is a typical process upon reducing the fully oxidized MoO_3, and has been extensively studied in the past decades.[3] These studies, which mainly focus on identifying crystalline phases employing X-ray radiation or electron emission as detection techniques, provide complex information including both the surface and bulk phase. In fact, the chemistry of several outermost layers of MoO_x, which is still a challenging task, is more meaningful for catalytic reactions that usually take place on a surface. Calculations have proposed models of surface defect sites, and have suggested that electrons left behind after oxygen removal could be confined or be localized in defect sites or oxygen vacancy sites.[4,5] We have employed probe reactions to investigate the surface properties of oxide catalysts, and have obtained precise surface information, such as acidity and basicity, at the identical level of contacted adsorbates, reactants, or sensing gas.[6] Inspired by this work, we endeavored to develop new strategies to detect and measure surface electrons, and to establish a structure–activity relationship. It turns out that confined electrons on the surface of reduced MoO_x are transferrable to the pertinent environment, and such electron transfer greatly depends on the reduction degree of MoO_x and the electron affinity of acceptors. Based on above results, we prepared negatively charged gold nanoparticles by depositing gold colloids on MoO_x and we evaluated their catalytic performance. We demonstrate herein that a profound knowledge of the state of electrons in surface defect sites is necessary to successfully understand catalysis mechanisms, and is in turn helpful in directing catalyst design.

The fully oxidized MoO_3 was prepared by calcining ammonium heptamolybdate in oxygen, and it was used as starting material. Reduction of MoO_3 was conducted in an atmosphere of 5% H_2 balanced with Ar gas at temperatures ranging from 200 °C to 480 °C. The numbers in the sample names, for example M390, indicate the reduction temperature, in this case 390 °C. Reactions between molybdenum oxides and electron acceptors were carried out in acetonitrile solution and were monitored by ultraviolet/visible (UV/Vis) spectroscopy.

We employed tetracyanoethylene (TCNE) as a probe molecule. The molecule has four cyano groups conjugated to the central C=C double bond with low-energy π* orbitals. The addition of an electron to TCNE produces an electron–TCNE complex ($TCNE^{\bullet-}$), the color of which is blue and can be quantitatively measured by UV/Vis spectroscopy. The absorption peak at about 330 nm signifying the formation of the blue anion radical of $TCNE^{\bullet-}$ is evidence of an electron-transfer reaction.[7,8] Both the fresh TCNE acetonitrile solution (Figure 1a) and the suspension solution with the fully oxidized MoO_3 (Figure 1b) did not show the absorption peak. When a partially reduced MoO_x (M390) was tested, the acetonitrile solution instantaneously changed color to blue. The maximum absorption peak was observed at 328 nm (Figure 1c), and was assigned to be $TCNE^{\bullet-}$,[7,8] indicating that the electron-transfer reaction had occurred. The sample reduced at 450 °C (M450) did not result in the absorption peak of $TCNE^{\bullet-}$, indicating that no electron is transferred to the TCNE molecule (Figure 1d).

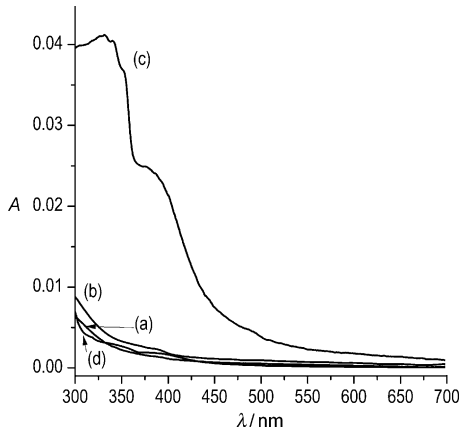

Figure 1. UV/Vis absorption spectra of TCNE solution. a) TCNE (1 g L^{-1}) in acetonitrile. b), c), d) Spectra of the solution in (a) after incubating the fully oxidized MoO_3, M390, and M450, respectively, for 10 min.

[*] Prof. Dr. F. Wang, Prof. Dr. J. Xu
State Key Laboratory of Catalysis, Dalian National Laboratory for Clean Energy, Dalian Institute of Chemical Physics
Chinese Academy of Sciences, Dalian 116023 (P. R. China)
E-mail: wangfeng@dicp.ac.cn
xujie@dicp.ac.cn
Prof. Dr. W. Ueda
Catalysis Research Center, Hokkaido University, Sapporo (Japan)

[**] The work was supported by the National Natural Science Foundation of China (Project 21073184) and One Hundred Person Project of the Chinese Academy of Sciences. We thank Dr. Dangsheng Su and Dr. Hans-Joachim Freund of Fritz-Haber-Institut der Max-Planck-Gesellschaft for their valuable suggestions in paper preparation.

Supporting information for this article is available on the WWW under http://dx.doi.org/10.1002/anie.201105922.

The above-mentioned results indicate that reduction condition is very important. When the reduction was conducted in the range of 350–410 °C, the solution color of TCNE changed to blue (Supporting Information, Figure S1). The maximum amount of transferable electrons was detected at 390 °C (M390; Figure 2). We believe that the temperature

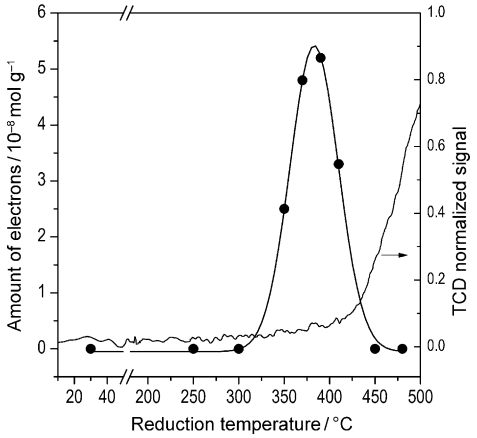

Figure 2. The effect of reduction temperature (200–480 °C) on the amount of transferable electrons. The results were measured by using the absorption peak of 330 nm in the UV/Vis spectra. The curve was simulated using a nonlinear Gauss fit.

range of 350–410 °C is critical to remove oxygen from MoO_3 and to maintain the bulk phase in an unreduced state. Upon reduction, the confined electron in the oxygen vacancy site is metastable, and therefore transferable once it contacts with adsorbed TCNE molecule. When the reduction temperature is increased to 410 °C, the confined electrons occupying the oxygen vacancy site redistribute (delocalize) to a neighboring Mo site because of the decrease in the Fermi level, resulting in Mo^{5+} or Mo^{4+}. As a result, the bulk phase is reduced, generating bulk oxygen vacancy sites and forming Mo suboxides or Magneli phases.[9] In our study, no evidence shows that electrons can be abstracted from Mo^{5+} or Mo^{4+} sites by electron acceptors. Some other reports suggest that bulk phase reduction started from about 400 °C.[3] Characterization by X-ray diffraction (XRD) indicates that the MoO_2 phase evolved from 410 °C (M410; see the Supporting Information, Figure S2d,e). At temperature less than 300 °C, no reduction of MoO_3 is observed, and the prolongation of reduction time (isothermal time) also does not lead to reduction. At temperatures of 350–410 °C, isothermal reduction for 0.5–6 h does not lead to further reduction; that is, no bulk reduction is observed. The supply of hydrogen (H_2/Mo^{6+} = 6:1) is abundant enough to reduce Mo^{6+} to Mo^{5+} or Mo^{4+}, indicating the process is not kinetically controlled. Temperature-programmed reduction (TPR) of the fully oxidized MoO_3 is conducted in an H_2/Ar atmosphere (Figure 2; for a detailed TPR profile, see the Supporting Information, Figure S3). Apparent hydrogen consumption is observed at 400 °C. Further increase in temperature leads to a deep reduction of the bulk phase, as indicated by a large amount of hydrogen consumption. These results are in good accordance with UV tests and XRD characterizations.

Isothermal reduction was conducted for 0.5 h. After the sample was cooled to room temperature, the sample color intensity did not change and the adsorption with TCNE still led to the blue color, indicating that these electrons confined in surface defect sites are not sensitive to the ambient atmosphere. The explanations will be given below.

Using the molar absorptivity value of 2.64 $L\,mol^{-1}\,cm^{-1}$ for $TCNE^{\bullet-}$,[10] the concentration of $TCNE^{\bullet-}$ in the M390 acetonitrile solution is calculated to be 8×10^{-8} $mol\,L^{-1}$. The amount of electrons withdrawn from M390 is 5.2×10^{-8} $mol\,g^{-1}$ (the concentration of M390 in acetonitrile is 1.5 $g\,L^{-1}$), which corresponds to one electron per eight surface Mo sites. The effect of reduction temperature on the amount of transferable electrons is shown in Figure 3. We employed a series of electron acceptors with electron affinities ranging

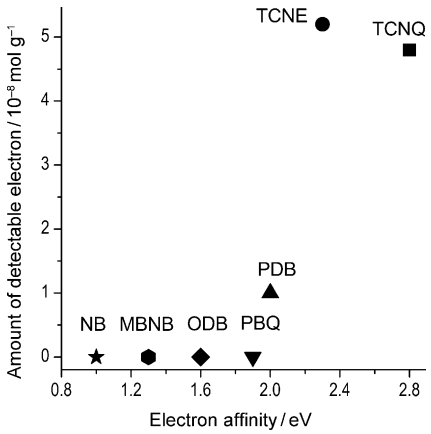

Figure 3. Amount of electrons at 390 °C detected by various electron acceptors. NB = nitrobenzene, MBNB = *m*-bromonitrobenzene, ODB = *o*-dinitrobenzene, PBQ = *p*-benzoquinone, PDB = *p*-dinitrobenzene, TCNE = tetracyanoethylene, TCNQ = tetracyano-*p*-quinodimethane.

from 1.0 eV to 2.8 eV (Figure 3). The results show that an electron can be abstracted by acceptors with larger electron affinity. The threshold value of electron affinity is about 2.0 eV, which can be viewed as the critical energy of exciting electrons from HOMO orbitals of oxygen vacancy sites (the Fermi level). Consequently, the stability of the reduced samples under ambient conditions is understandable because the electron affinity of molecular oxygen and water is 0.46 eV and 1.3 eV, respectively, which are too weak to form O_2^-[11,12] or hydrated electron (H_2O^-) species.[13] In this study, TCNE (2.3 eV) is an ideal probe molecule for studying surface defect sites. Although TCNQ has a larger electron affinity value (2.8 eV) than TCNE, the geometric hindrance probably restrains its adsorption on oxide surface, and hinders the electron-transfer process.

Electron transfer from MoO_x to electron acceptors attracted our interest in catalytic applications. It has been reported that an electron-rich environment, and especially organic ligands, such as nitrogen-containing polymers, is advantageous for selective oxidation reactions.[14,15] There-

fore, MoO_x could be regarded as a group of electron-rich inorganic ligands, and could be good candidate for a catalyst support. We prepared several gold catalysts using the same source of gold colloid as impregnation solution on the as-prepared MoO_x according to previous work,[16] and thus the size affect on different catalysts is eliminated. The gold colloid containing a uniform size of nanoparticles (ca. 3 nm) was prepared by reducing chloroauric acid with $NaBH_4$ (Supporting Information, Figure S4a,b). The study allows us to evaluate pure support effects on catalytic activity.

We studied the charge state of Au nanoparticles using XPS. The binding energy was corrected for surface charging by taking the C1s peak of contaminant carbon as a reference at 285.0 eV.[17] Figure 4a shows the XP spectra of Au/MoO_3, Au/M390, and Au/M450. The $Au\,4f_{7/2}$ binding energies of

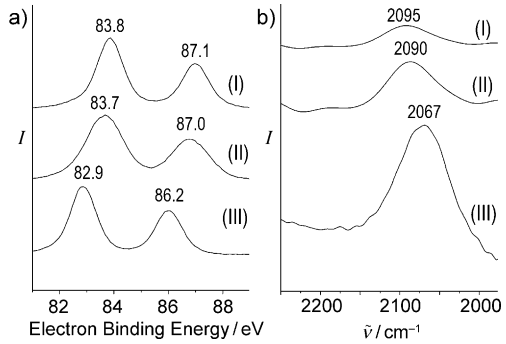

Figure 4. a) XPS and b) CO-FTIR spectra of the samples of (I) Au/MoO_3, (II) Au/M450, and (III) Au/M390.

these samples are 83.8, 83.7, and 82.9 eV, respectively. The $Au\,4f_{7/2}$ binding energy of Au/M390 is significantly smaller (82.9 eV) than that of the bulk gold film (84.0 eV). The −1.1 eV negative shift of the binding energy of $Au\,4f_{7/2}$ suggests that negative charges are deposited on Au, which is the result of electron transfer from oxygen vacancy sites. The −0.3 eV negative shift of the binding energies of $Au\,4f_{7/2}$ was reported for other supported Au particles and was explained in a similar manner.[14,18,19] The reason for electron transfer from oxide to gold nanoparticles is explained as the follows. Electron affinity of neutral gold particle is size-dependent.[20] When the size is remarkably decreased to less than about 5 nm, surface Au atoms on the nanoparticle behave more like a single Au atom, are highly active, and easily anionically ionized. The electron affinity of a single Au atom is 2.3 eV,[20] which is larger than the threshold value of electron transfer. The driving force for electron transfer from the oxide surface to Au atoms originates from surface conjugation and the differential Fermi energy level. It takes some charge to equalize the Fermi levels.[20,21]

CO-FTIR is a technique to probe charge state of supported Au particles.[22,23] Figure 4b shows the behavior of the CO adsorption band on Au/MoO_3, Au/M390, and Au/M450, respectively, in contact with 10 mbar of ^{12}CO at RT. As for Au/M390, the maximum ^{12}CO band is quite broad and significantly red-shifted to 2067 cm^{-1}; whereas the values for Au/MoO_3 and Au/M450 are 2095 cm^{-1} and 2090 cm^{-1}, respectively. The maximum band related to ^{12}CO is not far from the typical CO adsorption on neutral gold (2100 cm^{-1}). The spectroscopic features suggest that the adsorbing gold sites for Au/MoO_3 and Au/M450 are neutral gold particles, and for Au/M390 negatively charged gold particles. The red-shift of the CO band (2067 cm^{-1}) is due to the greater π back-donation from the negatively charged Au. Theoretically, a red-shift of the CO stretching frequency of 25 to 80 cm^{-1} depending on the charge on the gold clusters was predicted, which agrees rather well with our observed values.[24]

We employed the aerobic oxidation of alcohols as model reactions to test activities of Au/MoO_x catalysts. The fully oxidized MoO_3, M390, and M450 gave less than 15% conversion of benzyl alcohol (Table 1, entries 1–3). Doping the fully oxidized MoO_3 with gold particles gave 44% conversion of benzyl alcohol (Table 1, entry 4). An exceptional increase in the conversion of benzyl alcohol was observed over Au/M390. Nearly 100% conversion of benzyl alcohol and the 94% yield of benzaldehyde were obtained (Table 1, entry 5). In comparison, the yield of benzaldehyde was 29% over Au/M450 (Table 1, entry 6). The Au/M390

Table 1: Aerobic oxidation of various alcohols.[a]

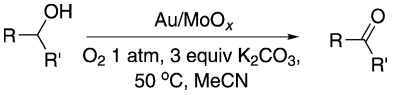

Entry	Catalyst[b]	S_{BET} [$m^2\,g^{-1}$]	Substrate	t [h]	Conv.[c] [%]	Yield[d] [%]
1	MoO_3	2.9	benzyl alcohol	10	11	–
2	M390	14.2	benzyl alcohol	10	14	–
3	M450	40.4	benzyl alcohol	10	10	–
4	Au/MoO_3	2.8	benzyl alcohol	10	44	–
5	Au/M390	13.9	benzyl alcohol	14	>99	94
6	Au/M450	39.0	benzyl alcohol	14	53	29
7	Au/M390	13.9	*p*-chlorobenzyl alcohol	16	>99	90
8	Au/M390	13.9	cyclohexanol	10	>99	93
9	Au/M390	13.9	2-phenylethanol	8	>99	94
10	Au/M390	13.9	1-butanol	20	>99	88
11	Au/M390	13.9	2-butanol	12	>99	92
12	Au/M390	13.9	1-hexanol	18	>99	87
13	Au/M390	13.9	2-hexanol	18	>99	85
14	Au/M390	13.9	1-octanol	15	>99	89
15	Au/M390	13.9	2-octanol	15	>99	90
16	Au/M390[e]	13.9	benzyl alcohol	14	11	–
17	Au/M390[f]	13.9	benzyl alcohol	14	>99	93
18	Au/M390[g]	13.9	benzyl alcohol	14	>99	92

[a] Typical reaction conditions: 5 mmol alcohol, 15 mmol K_2CO_3, 100 mg catalyst, 5 mL acetonitrile, 50°C. Experiments were conducted in a quartz reactor. Pure oxygen gas (1 atm) was supplied by a balloon. Samples were withdrawn at intervals to track the reaction by TLC. [b] M390 and M450 indicate that the catalyst supports were reduced in 5% H_2 balanced with Ar at 390°C and 450°C, respectively. The loading amount of Au was 1.1 wt% in all catalysts as analyzed by ICP-mass spectometry. [c] The conversion was determined by gas chromatography. [d] Products were isolated on silica gel using hexane/ethyl acetate (2.5:1) as effluent solution. [e] In the absence of K_2CO_3. [f] Air was used instead of pure oxygen. [g] The result of the third reuse.

could catalyze the oxidation of other primary or secondary alcohols to the corresponding aldehydes or ketones in high yields (Table 1, entries 7–15). The reaction did not occur in the absence of base (Table 1, entry 16). The oxidation under 1 atm air proceeded in a comparable result to that under 1 atm of pure oxygen (Table 1, entry 17), indicating that the reaction was not controlled by an oxygen mass-transfer process. After reaction, the Au/M390 catalyst was filtered out, washed with solvent, and reused. Catalytic results were stable over three cycles (Supporting Information, Figure S5). The yields of benzaldehyde were more than 90% in all reuse tests (Table 1, entry 18). The inductively coupled plasma (ICP) mass analysis revealed that no Au species content was detected in the reaction mixture, indicating the strong interaction between Au and support. The hot filtration test was conducted. No further conversion of benzyl alcohol was observed after catalyst was filtered out, indicating that the catalyst was heterogeneous in nature (Supporting Information, Figure S6). The great difference of catalysis is majorly attributed to a support effect, because of which M390 is able to transfer electrons to the Au nanoparticles. It was reported by Tsunoyama et al. that the catalytic activity of Au for aerobic oxidations is enhanced by an increase in the amount of negative charge on the Au core.[14,25] The size effect on catalysis can be neglected since the size of gold particle in all of the catalysts was the same, as characterized by TEM before and after reaction. The increased catalytic activity is not due to specific surface area, as Au/M450 (39.0 $m^2 g^{-1}$) has a larger surface area than Au/M390 (13.9 $m^2 g^{-1}$).

A linear relationship exists between $-\ln(1-C)$ and reaction time (ks), indicating that the reaction is first order with respect to benzyl alcohol as shown in Figure 5a. H/D kinetic isotope effects (KIE) for the oxidation of benzyl alcohol and α-deuterated benzyl alcohol was evaluated. The rate constant k_H for $PhCH_2OH$ at 50 °C was 7.7×10^{-5} s^{-1} and for $PhCD_2OH$ $k_D = 1.4 \times 10^{-5}$ s^{-1}. A large value of k_H/k_D (5.5) at 50 °C was observed. It can be inferred from the KIE result that the cleavage of the C–H bond at benzylic position is the rate-determining step. The apparent activation energy, E_a, associated with the C–H bond cleavage is determined from the Arrhenius plot in the temperature range of 40–70 °C (Figure 5b). The least-square fit analysis yields E_a values of 28.1 kJ mol^{-1}, which is smaller than the reported values of 45.7 kJ mol^{-1},[26] 45.8 kJ mol^{-1} [27] and 32.3 kJ mol^{-1}.[28]

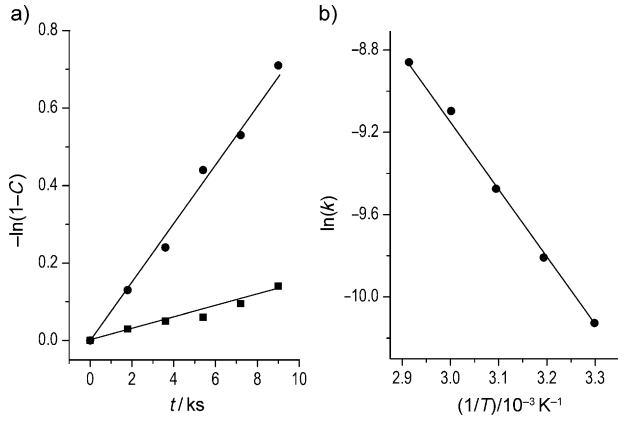

Figure 5. a) Time-on-stream course of conversion. ● $PhCH_2OH$, ■ $PhCD_2OH$. C = conversion of benzyl alcohol. b) Arrhenius plot for the oxidation of $PhCH_2OH$.

The catalysis mechanism is considered as the follows. Partial reduction of the fully oxidized MoO_3 generates surface defect sites. Electrons are localized in oxygen vacancy sites after oxygen removal. These electrons transfer to the supported gold nanoparticles, depositing there negative charges, which are responsible for the formation of active oxygen species, for example superoxo- or peroxo-like species.[14,17] A β-hydrogen atom abstraction from alcohol generates corresponding aldehydes or ketones. The catalytic results of Au/MoO_x are likely relevant to other oxide-supported Au catlyatst, such as Au/MgO, Au/TiO_2 and Au/PVP.

In summary, we employed single electron oxidants as electron acceptors to investigate surface defect sites on partially reduced molybdenum oxides. We detected free electrons in surface defect sites and quantitatively measured the threshold value of electron transfer. Our studies show that partially reduced molybdenum oxides can transfer electrons to the pertinent environment. Such electron transfer deposits negative charges on the closely contacted Au nanoparticles, which explains high catalytic activities in the aerobic oxidation of alcohols. We believe that the study will greatly contribute to the knowledge of electron states of surface defect sites of oxides and their catalytic applications.

Received: August 22, 2011
Revised: January 9, 2012
Published online: March 13, 2012

Keywords: defect sites · electron transfer · heterogeneous catalysis · molybdenum oxides · oxidation

[1] a) M. P. House, A. F. Carley, M. Bowker, *J. Catal.* **2007**, *252*, 88–96; b) T. Ressler, A. Walter, Z. D. Huang, W. Bensch, *J. Catal.* **2008**, *254*, 170–179; c) T. Ressler, A. Walter, J. Scholz, J. P. Tessonnier, D. S. Su, *J. Catal.* **2010**, *271*, 305–314; d) M. Bowker, M. P. House, A. F. Carley, *J. Catal.* **2007**, *252*, 88–96; e) F. Wang, W. Ueda, *Chem. Commun.* **2009**, 1079–1081.

[2] a) A. S. K. Hashmi, G. J. Hutchings, *Angew. Chem.* **2006**, *118*, 8064–8105; *Angew. Chem. Int. Ed.* **2006**, *45*, 7896–7936; b) M. V. Ganduglia-Pirovano, C. Popa, J. Sauer, H. Abbott, A. Uhl, M. Baron, D. Stacchiola, O. Bondarchuk, S. Shaikhutdinov, H.-J. Freund, *J. Am. Chem. Soc.* **2010**, *132*, 2345–2349; c) N. Soultanidis, W. Zhou, A. C. Psarras, A. J. Gonzalez, E. F. Iliopoulou, C. J. Kiely, I. E. Wachs, M. S. Wong, *J. Am. Chem. Soc.* **2010**, *132*, 13462–13471; d) H.-J. Zhai, X.-H. Zhang, W.-J. Chen, X. Huang, L.-S. Wang, *J. Am. Chem. Soc.* **2011**, *133*, 3085–3094; e) X. Lin, B. Yang, H.-M. Benia, P. Myrach, M. Yulikov, A. Aumer, M. A. Brown, M. Sterrer, O. Bondarchuk, E. Kieseritzky, J. Rocker, T. Risse, H.-J. Gao, N. Nilius, H.-J. Freund, *J. Am. Chem. Soc.* **2010**, *132*, 7745–7749; f) J. Graciani, A. Nambu, J. Evans, J. A. Rodriguez, J. F. Sanz, *J. Am. Chem. Soc.* **2008**, *130*, 12056–12063; g) J. Guzman, S. Carrettin, J. C. Fierro-Gonzalez, Y. Hao, B. C. Gates, A. Corma, *Angew. Chem.* **2005**, *117*, 4856–4859; *Angew. Chem. Int. Ed.* **2005**, *44*, 4778–4781.

[3] a) T. Konig, G. H. Simon, H. P. Rust, G. Pacchioni, M. Heyde, H. J. Freund, *J. Am. Chem. Soc.* **2009**, *131*, 17544–17545; b) O. Kirilenko, F. Girgsdies, R. E. Jentoft, T. Ressler, *Eur. J. Inorg. Chem.* **2005**, 2124–2133; c) E. Lalik, W. I. F. David, P. Barnes,

J. F. C. Turner, *J. Phys. Chem. B* **2001**, *105*, 9153 – 9156; d) T. Leisegang, A. A. Levin, J. Walter, D. C. Meyer, *Cryst. Res. Technol.* **2005**, *40*, 95 – 105; e) R. Tokarz-Sobieraj, K. Hermann, M. Witko, A. Blume, G. Mestl, R. Schlogl, *Surf. Sci.* **2001**, *489*, 107 – 125; f) D. Wang, D. S. Su, R. Schlogl, *Z. Anorg. Allg. Chem.* **2004**, *630*, 1007 – 1014.

[4] M. V. Ganduglia-Pirovano, A. Hofmann, J. Sauer, *Surf. Sci. Rep.* **2007**, *62*, 219 – 270.

[5] E. Giamello, M. Chiesa, M. C. Paganini, D. M. Murphy, C. Di Valentin, G. Pacchioni, *Acc. Chem. Res.* **2006**, *39*, 861 – 867.

[6] a) F. Wang, W. Ueda, *Chem. Eur. J.* **2009**, *15*, 742 – 753; b) F. Wang, W. Ueda, *Top. Catal.* **2008**, *50*, 90 – 97.

[7] S. Sugunan, G. D. Rani, K. B. Sherly, *React. Kinet. Catal. Lett.* **1991**, *43*, 375 – 380.

[8] H. F. Askal, *Talanta* **1997**, *44*, 1749 – 1755.

[9] G. Pacchioni, *Theory of point defects at the MgO surfaces*, Elsevier Science, Dordrecht, **2001**, pp. 94 – 135,.

[10] A. M. El-Brashy, M. E. S. Metwally, F. A. El-Sepai, *Bull. Korean Chem. Soc.* **2004**, *25*, 365 – 372.

[11] M. Urban, M. Sulka, M. Pitonak, P. Neogrady, *Int. J. Quantum Chem.* **2008**, *108*, 2159 – 2171.

[12] S. J. Nalley, R. N. Compton, *Chem. Phys. Lett.* **1971**, *9*, 529 – 533.

[13] R. E. Ballard, *Chem. Phys. Lett.* **1972**, *16*, 300 – 301.

[14] H. Tsunoyama, N. Ichikuni, H. Sakurai, T. Tsukuda, *J. Am. Chem. Soc.* **2009**, *131*, 7086 – 7093.

[15] B. E. Salisbury, W. T. Wallace, R. L. Whetten, *Chem. Phys.* **2000**, *262*, 131 – 141.

[16] M. Comotti, W. C. Li, B. Spliethoff, F. Schuth, *J. Am. Chem. Soc.* **2006**, *128*, 917 – 924.

[17] E. D. Park, J. S. Lee, *J. Catal.* **1999**, *186*, 1 – 11.

[18] S. Arrii, F. Morfin, A. J. Renouprez, J. L. Rousset, *J. Am. Chem. Soc.* **2004**, *126*, 1199 – 1205.

[19] A. Roldán, J. M. Ricart, F. Illas, G. Pacchioni, *J. Phys. Chem. C* **2010**, *114*, 16973 – 16978.

[20] a) J. A. Smith, M. Josowicz, M. Engelhard, D. R. Baer, J. Janata, *Phys. Chem. Chem. Phys.* **2005**, *7*, 3619 – 3625; b) P. Pyykkö, *Angew. Chem.* **2004**, *116*, 4512 – 4557; *Angew. Chem. Int. Ed.* **2004**, *43*, 4412 – 4456.

[21] S. W. Boettcher, N. C. Strandwitz, M. Schierhorn, N. Lock, M. C. Lonergan, G. D. Stucky, *Nat. Mater.* **2007**, *6*, 592 – 596.

[22] M. Sterrer, M. Yulikov, E. Fischbach, M. Heyde, H.-P. Rust, G. Pacchioni, T. Risse, H.-J. Freund, *Angew. Chem.* **2006**, *118*, 2692 – 2695; *Angew. Chem. Int. Ed.* **2006**, *45*, 2630 – 2632.

[23] G. Pacchioni, P. S. Bagus, *J. Phys. Conf. Ser.* **2008**, *117*, 12003 – 12003.

[24] H. Hakkinen, B. Yoon, U. Landman, A. S. Worz, J. M. Antonietti, S. Abbet, K. Judai, U. Heiz, *Science* **2005**, *307*, 403 – 407.

[25] Y. Zhu, H. F. Qian, B. A. Drake, R. C. Jin, *Angew. Chem.* **2010**, *122*, 1317 – 1320; *Angew. Chem. Int. Ed.* **2010**, *49*, 1295 – 1298.

[26] F. Wang, W. Ueda, *Appl. Catal. A* **2008**, *346*, 155 – 163.

[27] G. J. Hutchings, D. I. Enache, J. K. Edwards, P. Landon, B. Solsona-Espriu, A. F. Carley, A. A. Herzing, M. Watanabe, C. J. Kiely, D. W. Knight, *Science* **2006**, *311*, 362 – 365.

[28] R. N. Ram, M. K. Dalal, M. J. Upadhyay, *J. Mol. Catal. A* **1999**, *142*, 325 – 332.

